ISBN: 978-3-95450-227-1 ISSN: 2673-5490 doi:10.18429/JACoW-IPAC2022-MOPOMS019

THE NEW SPARC_LAB RF PHOTO-INJECTOR

D. Alesini, M.P. Anania, A. Battisti, M. Bellaveglia, A. Biagioni, F. Cardelli, G. Costa, E. Chiadroni, M. Del Franco, G. Di Pirro, G. Di Raddo, L. Faillace, M. Ferrario, G. Franzini, A. Gallo, A. Giribono, A. Liedl, V. Lollo, L. Pellegrino, L. Piersanti, R. Pompili, S. Romeo, L. Sabbatini, V. Shpakov, A. Stella, C. Vaccarezza, A. Vannozzi, F. Villa
INFN-LNF, Frascati, Italy
M. Carillo, Sapienza University of Rome, Rome, Italy
A. Cianchi, M. Galletti, University of Tor Vergata, Rome, Italy

Abstract

A new RF photo-injector has been designed, realized and successfully installed at the SPARC_LAB facility (INFN-LNF, Frascati, Rome). It is based on a 1.6 cell RF gun fabricated with the new brazing-free technology, recently developed at the INFN-LNF. The electromagnetic design has been optimized to have a full compensation of the dipole and quadrupole field components introduced by the coupling hole, with an improvement of the effective pumping speed with two added pumping ports. The gun is over coupled (β=2) to reduce the filling time and to allow the operation with short RF pulses. The overall injector integrates a new solenoid with a remote control of the transverse position and a variable skew quadrupole for the compensation of residual quadrupole field components. It also allows an on axis laser injection with the last mirror in air, and the possibility of a future integration of an X/C band cavity linearizer. In the paper we report the main characteristics of the injector with particular focus on the new gun realization and final performances.

INTRODUCTION

The new injector of the SPARC_LAB Facility [1] is shown in Fig. 1. It is a complex system and has been designed to substitute the previous injector that had limitations in term of rf gun breakdown activity, solenoid alignment, laser mirror in vacuum and possibility of further improvements with the insertion of an X/C band linearizer. The injector integrates several new components, as illustrated in the next paragraph. In particular, the rf gun has been realized with the new brazing-free technology developed at INFN-LNF [2] and already adopted for the realization of new rf photo-guns [3, 4]. This technology has been demonstrated to exhibit very good performances in term of breakdown rates (BDR) and conditioning time, with a contemporary reduction of the cost and realization time. In the present paper, after a description of the overall photo-injector, we illustrate the new RF gun design, realization and performances showing preliminary measurements with beam.

NEW PHOTO-INJECTOR LAYOUT

The new injector is a complex system and integrates several different components, as given in Figs. 1 and 2 where the picture of the injector and mechanical section are reported. In particular, we have the already mentioned rf gun, the solenoid [5] with a remote control of its transverse position with a precision better than ±10 μm, the laser injection chamber that allows a laser injection with the last mirror in air, a complete diagnostic station with faraday cup, YAG screen and toroid, a skew quadrupole with variable polarity, embedded in the solenoid, for the tuning of the x-y emittances and compensation of residual asymmetries, and a corrector magnet for trajectory optimization and beam energy measurements. The injector allows also to insert, in the future, an X/C band linearizer.

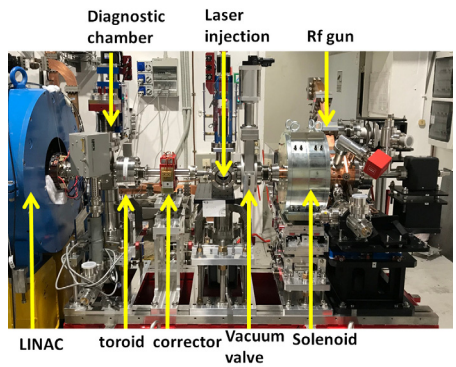

Figure 1: Picture of the new SPARC_LAB injector.

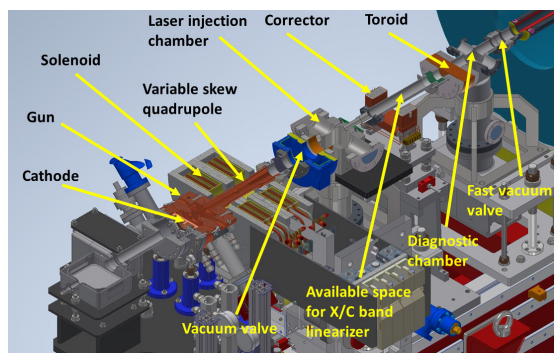

Figure 2: Mechanical section of the new photo-injector with main components.

THE NEW GUN

The gun integrates several new features both from the electromagnetic (e.m.) and the mechanical point of view. The e.m. design has been accomplished using ANSYS-HFSS [6] and the e.m. model is given in Fig. 3. It has been designed with three added holes in the coupling cell for a perfect compensation of the dipole and quadrupole e.m. field components introduced by the rf coupling hole.

The holes have been also connected to vacuum pumps allowing a strong improvement of the vacuum pressure

ISBN: 978-3-95450-227-1 ISSN: 2673-5490 doi:10.18429/JACoW-IPAC2022-MOPOMS019

that, in operation, is of few 10^{-10} mbar with a constant improvement. The effect of the added holes for the compensation of the quadrupole e.m. field components is well illustrated in Fig. 4 where we have reported the azimuthal magnetic field on three different arcs in the center of the coupling cell and the related quadrupole gradient as a function of the longitudinal position.

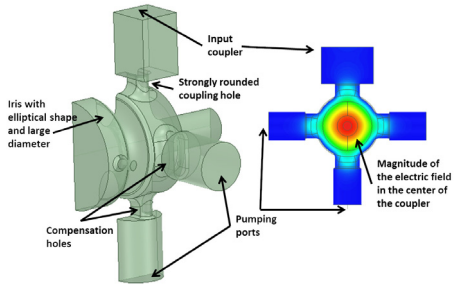

Figure 3: Electromagnetic model of the gun.

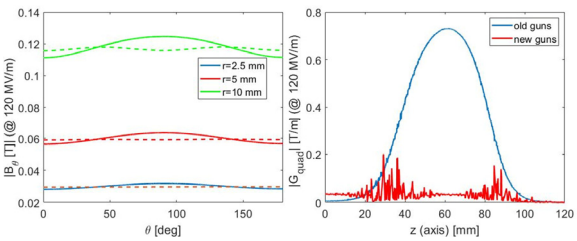

Figure 4: (left) Azimuthal magnetic field on three arcs in the center of the coupling cell; (right) quadrupole gradient as a function of the longitudinal position.

The gun has been designed with a coupling coefficient equal to 2 to allow operation with short rf pulses (<1μs) thus reducing the BDR and the power dissipation. An elliptical profile of the iris with large aperture (ϕ=36 mm) has been also implemented to reduce the peak electric field, to increase the 0-π mode frequency separation (thus avoiding excitation of the 0 mode with short rf pulses) and to obtain a better pumping speed on the cathode cell. The final rf gun parameters are reported in Table 1.

Table 1: Main Parameters of the New SPARC_LAB RF Gun (the values in parenthesis are those measured)

Parameter	value
Resonant frequency [GHz]	2.856 (2.856)
$E_{cath}/\sqrt{P_{diss}}$ [MV/(m·MW$^{0.5}$)]	37.5
RF input power [MW]	15
Cathode peak field [MV/m]	120
Rep. rate [Hz]	10
Quality factor	14300 (13900)
Filling time [ns]	515
Coupling coefficient	2 (1.99)
RF pulse length [μs]	1
Mode separation 0-π [MHz]	41 (41)
E_{surf}/E_{cath}	0.88
Pulsed heating [°C]	<30
Working temperature [°C]	25

GUN ASSEMBLY, LOW AND HIGH POWER RF TESTS

The realization technology without brazing allows to assemble the gun with special gaskets in a clean room and to proceed, after the vacuum test, directly to the rf characterization. Pictures of the gun under assembly and under rf test are given in Fig. 5. Measurements of the reflection at the input port (reported in Fig. 6) and transmission between the input port and the probe antenna have been performed. Electric field measurements with the bead drop technique have also been performed and are reported in Fig. 6.

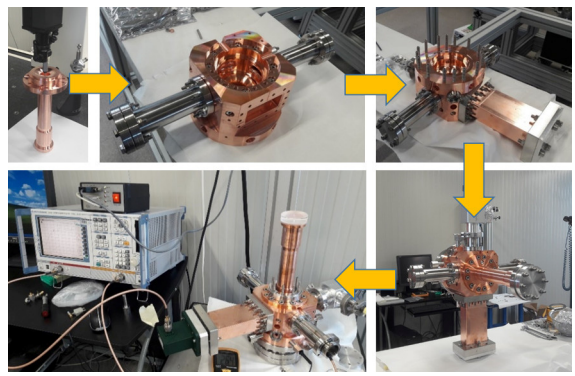

Figure 5: Pictures of the gun under assembly and under rf test.

After the low power rf characterization, the gun has been tested at high power, reaching the final performances (15 MW, 120 MV/m) in an incredible short time (less than 10 days at 10 Hz). The conditioning history is reported in Fig. 7 where the measured vacuum pressure, the rf input power and the pulse length have been reported. The conditioning has been done in a semi-automatic way looking at the vacuum behavior. In case of discharge and, as a consequence, vacuum level exceeding a given threshold (typically 5-6·10^{-8} mbar), the system automatically stopped rf power waiting for the vacuum recovering (typically 2-3·10^{-8} mbar) and restarted again with a reduction of the power of 0.1 dB. During the conditioning, we basically kept constant the repetition rate at 10 Hz, and we progressively increased the pulse length up to the nominal parameter. For each pulse length step, we increased the power level up to about 15 MW.

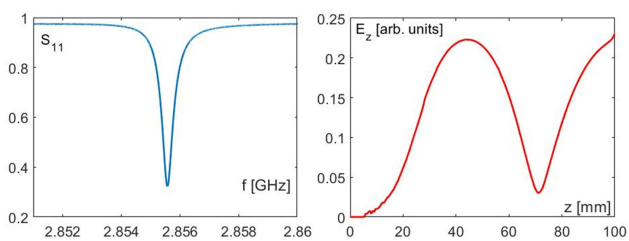

Figure 6: (left) Reflection coefficient at the input port; (right) measured electric field on axis.

During the injector conditioning (done on a parallel line with respect to its final installation) the solenoid was off. In total, during the 10 days of conditioning, ~5x10^6 pulses

ISBN: 978-3-95450-227-1 ISSN: 2673-5490 doi:10.18429/JACoW-IPAC2022-MOPOMS019

have been delivered to the gun with a total cumulated discharges less than 10^3. The final BDR has been measured in a 24-hour operation, as illustrated in the next paragraph. The gun has then been vented in dry nitrogen, moved in its final position and re-conditioned again also switching on the solenoid. The effect of these last two operations (venting and solenoid on) on the BDR were completely negligible and the gun recovered the final performances without any considerable effect.

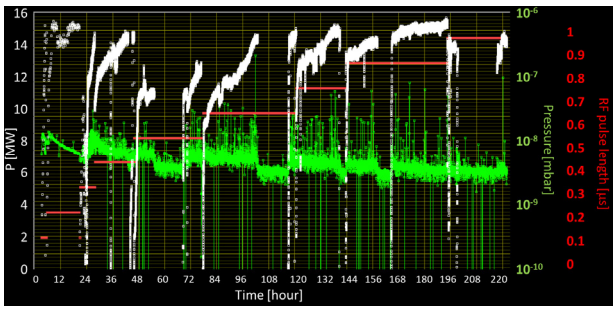

Figure 7: Gun conditioning history.

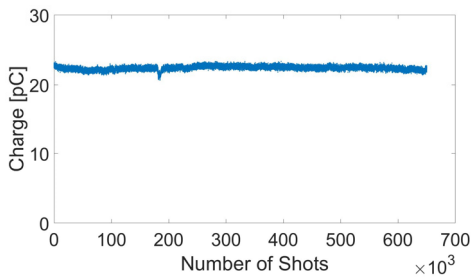

Figure 8: Measurements of the dark for 24 hour operation.

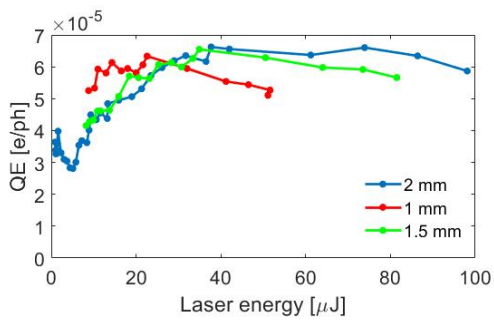

Figure 9: Measured quantum efficiency with different laser paramenters.

GUN PERFORMANCES WITH BEAM

The gun is currently, stably, in operation without breakdown activity. Several measurements have been performed: dark current, quantum efficiency, beam emittance, beam energy measurements and the complete description of the beam characterization and final beam quality will be the subject of a dedicated paper. Here we report, as an example, the measurements of the dark current at the diagnostic chamber (~1 m from the cathode) in a 24-hour operation (Fig. 8). Its value is constant at the level of about 22 pC and no discharges have been observed. Therefore, the BDR can be estimated to be below the 10^{-6} bpp level. The measured quantum efficiency with different laser parameters is reported in Fig. 9 and exceed the $5 \cdot 10^{-5}$ e/ph level (the decrease at low laser energy is under investigation and is probably due to a low sensitivity in the measurements). Lastly, the beam energy as a function of the input power is given in Fig. 10. In the same plot, the theoretical value is also reported.

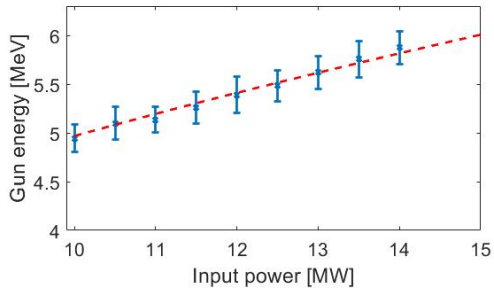

Figure 10: Beam energy as a function of the input power.

To deeply investigate the gun properties, simulations of the dark current have been also performed using the CST code [7]. The calculated spectrum of the dark current at 120 MV/m is reported in Fig. 11. The comparison between the measured values and the simulated one allows to calculate the effective enhancement factor β in the Fowler-Nordheim field emission expression also according to the general simulation parameters described, as example, in [8, 9]. Preliminary estimations give a β~95 and we have used, according to the mentioned papers, an effective area of the emitter A_e=0.01 μm^2.

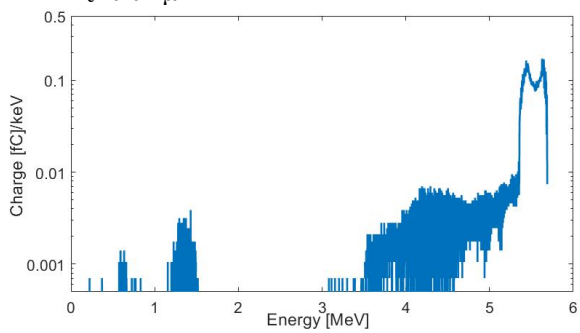

Figure 11: Calculated spectrum of the dark current.

CONCLUSIONS

In this paper we illustrated the main challenges of the new rf photo-injector for the SPARC_LAB facility. The overall new injector is a complex system and integrates several different components. In particular, the rf gun has been fabricated with the new technology w/o brazing and has been tested at high power showing extremely good performances in terms of conditioning time and final breakdown rates. The injector is now in operation and preliminary measurements have been shown.

ACKNOWLEDGEMENTS

We would like to acknowledge the DAΦNE-SPARC operators team. We would like also to acknowledge P. Chimenti, R. Di Raddo, S. Bini, B. Buonomo, C. Di Giulio and L. Foggetta for the technical support. The work has been partially supported by the Regione Lazio POR FESR 2014-2020.

ISBN: 978-3-95450-227-1 ISSN: 2673-5490 doi:10.18429/JACoW-IPAC2022-MOPOMS019

REFERENCES

[1] M. Ferrario *et al*., "SPARC_ LAB present and future," *Nucl. Instrum. Methods Phys. Res. B*, vol. 309, pp. 183-188, 2013.

[2] D. Alesini *et al*., International Patent Publication No. WO 2016/147118 A1, assigned to INFN.

[3] D. Alesini *et al*., "New technology based on clamping for high gradient radio frequency photogun," *Phys. Rev. ST Accel. Beams,* vol. 18, p. 092001, 2015.

[4] D. Alesini *et al*., "Design, realization, and high power test of high gradient, high repetition rate brazing-free S-band photogun," *PRAB 21*, p. 112001, 2018.

[5] A. Vannozzi *et al*., "Design and Realization of New Solenoids for High Brightness Electron Beam Injectors", in *Proc. IPAC'21*, Campinas, Brazil, May 2021, pp. 2374-2377. doi:10.18429/JACoW-IPAC2021-TUPAB366

[6] https://www.ansys.com/

[7] https://www.3ds.com/products-services/simulia/

[8] F. Cardelli *et al*., "Dark Current Studies for a High Gradient SW C-Band RF Gun", presented at IPAC'22, Bangkok, Thailand, Jun. 2022, paper MOPOMS020, this conference.

[9] T. G. Lucas, High Field Phenomenology in Linear Accelerators for the Compact Linear Collider, PhD Thesis, University of Melbourne, 2018.